

## Direct Sticking and Differential Adsorption Heats as Probes of Structural Transitions: O<sub>2</sub> on the Stepped Ni{211} Surface

Andrew D. Karmazyn, Vittorio Fiorin, and David A. King\*

Contribution from the Department of Chemistry, University of Cambridge, Lensfield Road, Cambridge, CB2 1EW, United Kingdom

Received May 14, 2004; E-mail: dak10@cam.ac.uk

**Abstract:** Coverage-dependent heats of adsorption and sticking probabilities for oxygen on Ni{211} have been measured at 300 K using single-crystal adsorption calorimetry. The data are consistent with a switch from dissociative chemisorption at low coverage to oxide formation above 2 ML adatom coverage. The initial heat of adsorption is 620 kJ mol<sup>-1</sup>, considerably higher than for any low Miller index nickel surface; this is attributed to the presence of low coordination step atoms that are preferably occupied up to 1 ML. As the coverage increases, the heat is found to drop very rapidly, indicating the presence of strong lateral adatom repulsions, which ultimately drive a transition from the chemisorption regime to oxide film formation at higher coverage. The shape of the coverage-dependent sticking probability is consistent with a direct adsorption mechanism at low coverage. At higher coverage, the transition between the chemisorption and oxidation regimes is relatively complex compared with low Miller index nickel surfaces. This is discussed in terms of the influence of the step sites on the {211} surface.

### 1. Introduction

The interaction of oxygen with the platinum group metal surfaces has been the subject of many theoretical and experimental studies,<sup>1–3</sup> due both to its importance in application areas such as catalysis and corrosion and in more fundamental aspects where, under controlled conditions, oxygen can undergo a variety of surface processes, from molecular to dissociative chemisorption, and from adsorption-induced surface reconstruction to surface oxidation. In addition, the behavior of molecules in the presence of surface defects in the form of steps or vacancies is of crucial importance if one wishes to understand chemical reactivity on “real” catalytic surfaces. One of the simplest stepped surfaces is the {211} surface, which is composed of two-atom-wide {111} terraces separated by a single-atom step of {001} orientation. Previous studies of the interaction of oxygen with this particular stepped surface have been mainly confined to Pt,<sup>3–6</sup> Cu,<sup>7–9</sup> and Au.<sup>10</sup> It is clear from these studies that the presence of steps plays a major role in oxygen adsorption. For example, in the case of Pt{211}, oxygen

dissociates on the step sites and the adatoms are bound in 2-fold bridge sites on the steps. On Cu{211}, using density functional theory (DFT), the adsorption of both molecular and dissociated oxygen has been shown to be enhanced by the presence of steps by some 0.2 eV for dissociation and by 0.4 eV for molecular adsorption, compared with the {111} surface.<sup>7,8</sup> On Au{111} and Au{211}, a similar DFT study has shown that oxygen does not adsorb on the {111} surface, whereas it adsorbs on the {211} surface with a binding energy of 0.15 eV,<sup>10</sup> again highlighting the enhancement of reactivity due to the step sites.

On nickel surfaces there have been many studies of the interaction of oxygen on low Miller index surfaces<sup>11</sup> but only a few studies on the stepped Ni surfaces.<sup>12–15</sup> It is pertinent therefore to extend these studies further in order to gain a broader understanding of the influence of steps in determining surface chemical reactivity. Furthermore, calorimetric measurements of the coverage-dependent differential heat of adsorption give a unique possibility to gain information on the energetics of irreversible processes, such as dissociative adsorption and surface oxidation.<sup>16,17</sup> Here, we report calorimetric results for the coverage-dependent heats of adsorption and sticking probabilities at room temperature of oxygen on Ni{211}, showing that the presence of step atoms is crucial in determining the adsorbate–surface structural transitions.

- (1) Hildebrandt, S.; Hagendorf, Ch.; Doege, T.; Jecksties, Ch.; Kulla, R.; Neddermeyer, H. *J. Vac. Sci. Technol. A* **2000**, *18*, 1010–1015.
- (2) Rose, M. K.; Borg, A.; Dunphy, J. C.; Mitsui, T.; Ogletree, D. F.; Salmeron, M. *Surf. Sci.* **2003**, *547*, 162–170.
- (3) Slijvancanin, Z.; Hammer, B. *Surf. Sci.* **2002**, *515*, 235–244.
- (4) Winkler, A.; Guo, X.; Siddiqui, H. R.; Hagans, P. L.; Yates Jr., J. T. *Surf. Sci.* **1988**, *201*, 419–433.
- (5) Gambardella, P.; Slijvancanin, Z.; Hammer, B.; Blanc, M.; Kuhnke, K.; Kern, K. *Phys. Rev. Lett.* **2001**, *87*, 056103-1, 4.
- (6) Siddiqui, H. R.; Winkler, A.; Guo, X.; Hagans, P. L.; Yates Jr., J. T. *Surf. Sci.* **1988**, *193*, L17–L23.
- (7) Xu, Y.; Mavrikakis, M. *Surf. Sci.* **2003**, *538*, 219–232.
- (8) Wang, Z. X.; Tian, F. H. *J. Phys. Chem. B* **2003**, *107*, 6153–6161.
- (9) Witte, G.; Braun, J.; Nowack, D.; Bartels, L.; Neu, B.; Meyer, G. *Phys. Rev. B* **1998**, *58*, 13224–13232.
- (10) Xu, Y.; Mavrikakis, M. *J. Phys. Chem. B* **2003**, *107*, 9298–9307.

- (11) Bolotin, I. L.; Kutana, A.; Makarenko, B.; Rabalais, J. W. *Surf. Sci.* **2001**, *472*, 205–222.
- (12) Pearl, T. P.; Darling, S. B.; Sibener, S. J. *Surf. Sci.* **2001**, *491*, 140–148.
- (13) Dorset, H. E.; Go, E. P.; Reutt-Robey, J. E.; Bartelt, N. C. *Surf. Sci.* **1995**, *342*, 261–271.
- (14) Martensson, A. S. *Surf. Sci.* **1989**, *215*, 55–64.
- (15) Kirstein, W.; Petraki, I.; Thieme, F. *Surf. Sci.* **1995**, *331*, 162–167.
- (16) Brown, W. A.; Kose R.; King, D. A. *Chem. Rev.* **1998**, *98*, 797–831.
- (17) Ge, Q. F.; Kose R.; King, D. A. *Adv. Catal.* **2000**, *45*, 207–259.

## 2. Experimental Section

The single crystal adsorption calorimeter (SCAC) has been described in detail previously<sup>18,19</sup> and here only a brief account of the experimental technique is given. Experiments were performed in an ultrahigh vacuum chamber with a base pressure of better than  $5 \times 10^{-11}$  Torr. Oxygen was dosed on Ni{211} at room temperature using a pulsed supersonic molecular beam. Each pulse, which consists of approximately  $2 \times 10^{12}$  molecules, is 50 ms in duration with a repetition period of 2.5 s. The intensity of the molecular beam is absolutely calibrated after each experiment by using a spinning rotary gauge. The Ni single crystal surface is in the form of a thin film (200 nm thick) in order to achieve a measurable change in temperature upon adsorption. The heat of adsorption is deduced by the temperature change that is remotely monitored via infrared radiation, using a mercury cadmium telluride (MCT) infrared detector and calibrated using a pulsed laser beam collimated through the molecular beam apertures. Typically the initial adsorption of a single gas pulse gives a temperature rise on the order of 0.1 K at the single-crystal thin film. In conjunction with heat measurements, sticking probability as a function of coverage is measured using the King and Wells method,<sup>20</sup> by measuring the portion of the incident gas pulse that is reflected from the surface.

It is well-known in single-crystal adsorption calorimetry that once saturation of the surface occurs, the amount of desorbing species between molecular beam pulses equals the incremental amount adsorbed in the preceding pulse, giving no net accumulation on the surface,<sup>16</sup> and the coverage scale may indefinitely extend. This is a “steady-state regime” for which the heat of adsorption and sticking probability remain approximately constant as the apparent coverage increases (i.e. with no net accumulation on the surface).

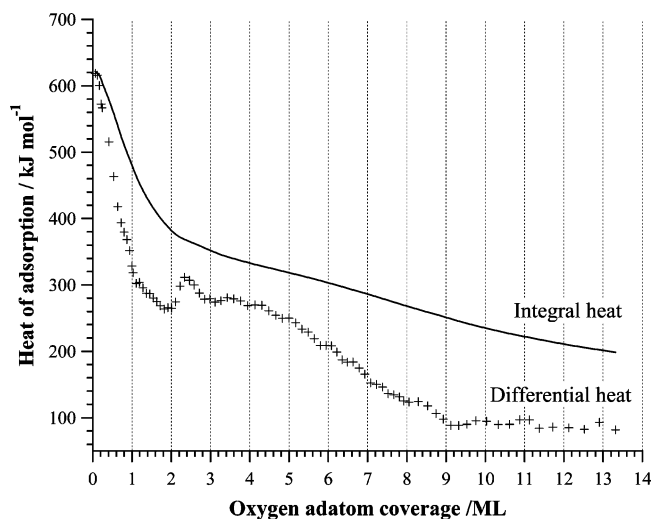
Cleaning of the Ni{211} surface consisted of cycles of gentle argon ion sputtering at discharge currents below  $8 \mu\text{A}$  and annealing at 700 K. Oxygen treatment using the molecular beam was also used to completely remove further contaminants. The cleanliness of the surface was checked by means of Auger electron spectroscopy (AES) and the structure by low energy electron diffraction (LEED).

Experimental data points of both the differential heat of adsorption and sticking probability result from an average of seven experimental runs.

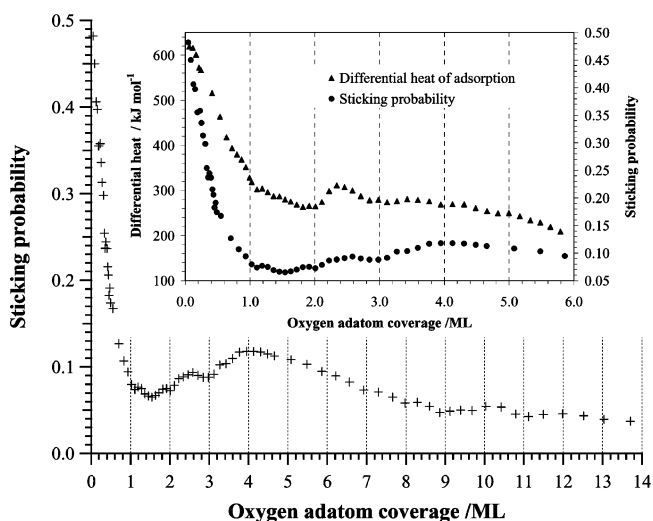
## 3. Experimental Results

Figure 1 shows the calorimetric differential heat of adsorption of O<sub>2</sub> on Ni{211} at room temperature as a function of oxygen coverage (1 ML coverage is defined as one oxygen adatom per  $(1 \times 1)$  {211} unit cell; there are  $6.57 \times 10^{14}$  unit cells  $\text{cm}^{-2}$ ). The integral heat derived from the data is also shown. Figure 2 shows the coverage-dependent sticking probability. The detailed behavior of the coverage dependence of the heat is unusual; the initial heat on the clean surface is  $620 \text{ kJ mol}^{-1}$ , and as the coverage increases, several regimes are distinguishable. For coverages up to 1 ML, the heat falls sharply to a value of  $300 \text{ kJ mol}^{-1}$ . This is followed by a less rapid linear decrease to a value of  $265 \text{ kJ mol}^{-1}$  for coverages up to 1.8 ML. At this point the heat increases in an unusual manner and then subsequently decreases over the coverage range 2–3 ML, exhibiting a maximum value of  $310 \text{ kJ mol}^{-1}$  at 2.3 ML. After this the heat remains constant at around  $270 \text{ kJ mol}^{-1}$  until 4 ML, where it begins to decrease to a steady-state value of  $90 \text{ kJ mol}^{-1}$  at a steady-state coverage of 9 ML.

The O<sub>2</sub> coverage-dependent sticking probability curve,  $s(\theta)$ , which is shown in Figure 2, also exhibits different regimes. From



**Figure 1.** Coverage dependence of the differential heat of adsorption (crosses) and integral heat of adsorption (solid line) for oxygen on Ni{211} at 300 K.



**Figure 2.** Coverage dependence of the sticking probability for oxygen on Ni{211} at 300 K. The inset shows an enlargement of both differential heat and sticking probability in the coverage range 0–6 ML.

an initial value of 0.5, it drops sharply in a linear fashion to a value of 0.17 at 0.5 ML coverage and less rapidly to 0.08 at 1 ML coverage. As the coverage increases further,  $s(\theta)$  exhibits a shallow minimum in the range between 1 and 2 ML and then increases in two steps, reaching a first maximum of 0.09 at 2.6 ML and a second of 0.12 at 4 ML. Subsequently, it falls gently until saturation at the steady-state regime occurs at 9 ML.

## 4. Discussion

The peculiar behavior of a maximum in the oxygen sticking probability as a function of coverage is indicative of an oxidation process.<sup>21</sup> The high differential heat of adsorption at low coverages is thermodynamically driven down by strong lateral interadsorbate interactions until it reaches the heat of oxide film formation, when the adlayer develops into an oxide film. As shown in the inset of Figure 2, the pronounced breaks observed in both the sticking probability and the heat curves are closely correlated. In particular, at 2 ML coverage a transition point

(18) Borroni-Bird, C. E.; King, D. A. *Rev. Sci. Instrum.* **1991**, *62*, 2177–2185.

(19) Stuck, A.; Wartnaby, C. E.; Yeo, Y. Y.; Stuckless, J. T.; Al-Sarraf, N.; King, D. A. *Surf. Sci.* **1996**, *349*, 229–240.

(20) King, D. A.; Wells, M. G. *Surf. Sci.* **1972**, *29*, 454–482.

(21) Stuckless, J. T.; Wartnaby, C. E.; Al-Sarraf, N.; Dixon-Warren, St. J. B.; Kovar, M.; King, D. A. *J. Chem. Phys.* **1997**, *106*, 2012–2030.

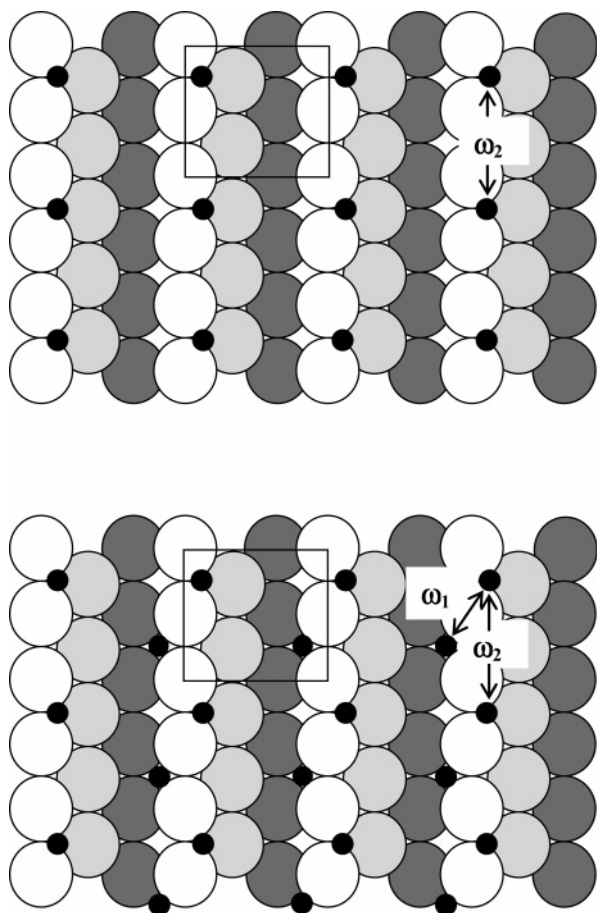


**Figure 3.** Schematic plan view of the proposed models for oxygen adatoms Ni{211} at (a) 0.5 ML and (b) 1 ML, based on DFT calculations.<sup>22</sup> The near-neighbor and the second-neighbor pairwise adatom–adatom interactions,  $\omega_1$  and  $\omega_2$ , derived from the heat measurements, are also shown here.

can be seen for which both the heat and the sticking probability begin to rise. One can therefore distinguish adsorption in a chemisorption regime for coverages up to 2 ML and in the oxide film growth regime for coverages greater than 2 ML.

**4.1. Adsorption in the Chemisorption Regime.** The high values of the heat of adsorption of oxygen at room temperature are clearly indicative of dissociative adsorption. The same ( $2 \times 1$ ) LEED pattern is observed at 0.5 and 1 ML, which is consistent with oxygen adatoms occupying step atoms, as shown in Figure 3a,b. To assign adsorption sites occupied by O adatoms on Ni{211}, we make use of preliminary density functional theory (DFT) calculations performed by our group. These calculations are consistent with the initial adsorption occurring on the steps.<sup>22</sup> The most favorable adsorption site is found to be the 3-fold site involving two step atoms and one terrace atom at a coverage corresponding to a single adatom in a ( $2 \times 1$ ) unit cell, i.e., 0.5 ML. The second, third, and fourth most favorable adsorption sites are also associated with steps. The second and third are equal in energy, involving a bridge site on the step and a 3-fold site between one step atom and two terrace atoms, respectively. The fourth most favorable adsorption site is a 4-fold site on the step edge. Figure 3b, for 1 ML coverage, makes the simple assumption that a further site with the same symmetry is occupied at 1 ML to again repeat the ( $2 \times 1$ ) LEED pattern.

(22) Jenkins, S. J. Private communication.

**Table 1.** Comparison of Data Pertaining to the Interaction of Oxygen with Nickel Surfaces in the Chemisorption Regime<sup>a</sup>

|                      | $q_0/\text{kJ mol}^{-1}$ | $s_0$ | $E_b/\text{kJ mol}^{-1}$ |
|----------------------|--------------------------|-------|--------------------------|
| Ni{211} <sup>b</sup> | 620                      | 0.48  | 557                      |
| Ni{100} <sup>c</sup> | 550                      | 0.63  | 520                      |
| Ni{110} <sup>c</sup> | 475                      | 0.78  | 485                      |
| Ni{111} <sup>c</sup> | 440                      | 0.23  | 470                      |

<sup>a</sup>  $q_0$  is the initial differential heat of adsorption,  $s_0$  is the initial sticking probability, and  $E_b$  is the O–Ni bond energy derived from  $\text{O}_2(\text{g}) + \text{Ni} \rightarrow 2\text{O}_{\text{Ad}}/\text{Ni}$  and  $\text{O}_{\text{Ad}}/\text{Ni} \rightarrow \text{O}(\text{g})$  at the lowest coverage. <sup>b</sup> This work. <sup>c</sup> Data reproduced from ref 21.

The initial heat of adsorption,  $620 \text{ kJ mol}^{-1}$ , is considerably higher than the initial heat on any low index Ni surfaces. Initial adsorption heats for oxygen on the {100}, {110}, and {111} nickel surfaces are 550, 475, and 440  $\text{kJ mol}^{-1}$ , respectively.<sup>21</sup> This reflects the higher adsorption heat on the most uncoordinated atoms of the {211} surface. Clearly the presence of low-coordination step atoms makes adsorption energetically more favorable. The sticking probability curve (Figure 2) also strongly suggests that dissociation occurs with a high sticking probability on direct impact, yielding  $s_0 = 0.5$  at the step sites, compared with the previously obtained value of  $s_0 = 0.23$  for the {111} surface,<sup>21</sup> which corresponds to the terrace structure on the present surface. The O–Ni surface bond strength is simply derived from the initial heat of adsorption and the molecular O–O bond dissociation energy of  $494 \text{ kJ mol}^{-1}$ , giving  $557 \text{ kJ mol}^{-1}$ . Table 1 reports the key values for oxygen adsorption in the chemisorption regimes in comparison with those obtained for adsorption on low Miller index Ni surfaces.

At 0.5 ML coverage, which corresponds to one oxygen adatom every two {211} unit cells, the differential heat has fallen to  $460 \text{ kJ mol}^{-1}$ , indicating strong lateral interactions between adsorbates. The magnitude of this interaction,  $\omega_2$ , shown in Figure 3a can be estimated by assuming that each oxygen adatom interacts with two other adatoms along the steps:

$$\omega_2 = (620 - 460)/(2 \times 2) = 40 \text{ kJ mol}^{-1}$$

The factor of 2 in the denominator accounts for fact that the measured heat of adsorption is per oxygen molecule. A pairwise repulsive interaction of  $40 \text{ kJ mol}^{-1}$  is a relatively high value, particularly at the O–O separation of  $4.98 \text{ \AA}$ . It is consistent with the fact that an ordered structure along the steps is observed by LEED at 0.5 ML, as shown in Figure 3a. As already mentioned, the same ( $2 \times 1$ ) pattern is also observed at 1 ML. At this coverage all the step atoms are saturated (i.e., one oxygen atom every unit cell, as shown in Figure 3b) and the differential heat of adsorption has further dropped to around  $300 \text{ kJ mol}^{-1}$ . This implies that saturation of steps requires a further energy cost in terms of interadsorbate interactions. Assuming that a second pairwise lateral interaction energy  $\omega_1$  corresponding to near-neighbor interactions can be independently invoked at 1 ML in addition to  $\omega_2$  (Figure 3b), this energy  $\omega_1$  can be estimated by considering only first neighbor interactions:

$$\omega_1 = (460 - 300)/(2 \times 2) = 40 \text{ kJ mol}^{-1}$$

This corresponds to an O–O distance of  $3.45 \text{ \AA}$ . While the magnitude of  $\omega_1$  for this system is the same as that reported for the  $c(2 \times 2)$ -O overlayer on Ni{100}, i.e.,  $40 \text{ kJ mol}^{-1}$ ,<sup>21</sup> where the O–O distance is  $3.52 \text{ \AA}$ , and hence also very similar,

a similar value for  $\omega_2$  at a significantly larger spacing, 4.98 Å, is surprising.

The fact that the interadsorbate lateral interactions are already strongly repulsive at 1 ML coverage means that repulsion for adsorption into any other site on the steps at higher coverage would be prohibitively high. The Pauli repulsion between filled O 2p<sub>x</sub> and 2p<sub>y</sub> orbital states would be far too strong, as clearly demonstrated by Ge and co-workers for oxygen adatoms on Pt{100}.<sup>23</sup> Further work is required to evaluate fully the nature of the repulsive interactions invoked here. We note that  $\omega_1$  involves each Ni atom in bond sharing to a given O atom. This effect is known as the bonding competition effect.<sup>24,25</sup> The appropriate surface d-bands of the Ni step edge atoms are stabilized in energy once bonding has occurred to the first oxygen adatom, and therefore, there is an energy cost in forming an additional bond with the second oxygen atom. In the case of Ni{100}, oxygen bonds in the 4-fold site and bond sharing also occurs. However, each nickel atom in the {100} case contributes to a quarter of the total bond with oxygen, whereas in the case of the stepped surfaces, each nickel atom contributes on average to more than a quarter of the bond. Therefore, qualitatively one can say that the valence bands of the nickel atoms are less stabilized on the {100} surface once the first oxygen bond is formed compared with the stepped surface. The substantial value of  $\omega_2$  at a larger O–O separation is clearly the result of the presence of step atoms, where the oxygen adatoms bond more favorably.

The corresponding heat of adsorption found by DFT at 0.5 ML is 490 kJ mol<sup>-1</sup>.<sup>22</sup> This value must be compared with the experimental integral heat of adsorption  $q_{\text{int}}(\theta)$  at 0.5 ML through the relationship

$$q_{\text{int}}(\theta) = \frac{\int_0^\theta q_{\text{diff}}(\theta') d\theta'}{\int_0^\theta d\theta'}$$

where  $q_{\text{diff}}(\theta)$  is the experimental differential heat. The coverage-dependent integral heat of adsorption is shown in Figure 1. For a coverage of 0.5 ML, we obtain a value of 560 kJ mol<sup>-1</sup>. The theoretical value is in fair agreement with the experimental value, noting that in the case of dissociative chemisorption of O<sub>2</sub> on Ni{111}, DFT calculations also slightly underestimate the heat of adsorption, by approximately 35 kJ mol<sup>-1</sup>.<sup>26</sup>

As the coverage increases between 1 and 2 ML, a clear change in the slope of the heat and sticking probability curves can be seen. It is reasonable to speculate that adsorption occurs on the terraces over this coverage range. This is consistent with the heat of adsorption of O<sub>2</sub> on Ni{111}, since the terraces of the {211} surface are of {111} character: extrapolating the heat in this coverage range (1–2 ML) to zero coverage, the initial value of ~400 kJ mol<sup>-1</sup> quite closely resembles the initial value of the adsorption heat reported for O<sub>2</sub> on Ni{111} (430 kJ mol<sup>-1</sup>).<sup>21</sup>

**4.2. Adsorption in the Oxidation Regime.** At coverages greater than 2 ML, the differential heat increases, coinciding

with the onset of oxidation, which is also revealed in the shape of the sticking probability curve,  $s(\theta)$ , in Figure 2. The increase in sticking probability for coverages greater than 2 ML is typical of a switch from chemisorption to oxidation, as previously observed for every low Miller index Ni surface.<sup>21</sup> Subsequently it reaches a maximum and then decreases. This behavior is consistent with the original work of Horgan and King<sup>27</sup> and the model proposed by Holloway and Hudson,<sup>28</sup> in which oxidation begins at nucleation points on the surface and proceeds by island growth. As the island boundaries get larger, the uptake rate increases and so too the sticking probability. However, as the coverage increases, the islands merge together and the length of the island boundaries progressively diminishes and the sticking probability approaches zero. This behavior explains the maximum in the sticking probability versus coverage, as also observed on low Miller index nickel surfaces.<sup>21</sup> In the case of the present work, a close inspection of the sticking probability reveals that in the oxidation regime  $s(\theta)$  exhibits a plateau in the coverage range of 2.4–3.0 ML. The corresponding heat of adsorption in the same coverage range falls and subsequently remains almost constant until 5 ML (as also shown in the inset in Figure 2). This feature of a falling heat in the oxidation regime was not observed on the low index Ni surfaces, and therefore it seems to be peculiar to the stepped Ni surface. A possible explanation for the decrease in the heat at 2.4 ML can be given by assuming a metastable regime in which oxidation and chemisorption are competitive mechanisms over the coverage range 2–3 ML. In this picture it is assumed that oxidation starts at nucleation points on the step atoms, and as the islands grow, adatoms from the terrace sites might be incorporated into the Ni–O layer. This process would generate clean terrace sites where chemisorption may occur. The resulting heat of adsorption would then drop in a fashion closely resembling the chemisorption regime at the terraces. This explanation is also supported by a LEED and STM study of O<sub>2</sub> on a vicinal Ni{100} surface,<sup>29</sup> which exposes terraces of 100 Å width separated by monatomic steps. This study revealed that Ni–O crystallites preferentially start to grow at the step edges. In addition, from the STM images there appear to be no adatoms closely surrounding the oxide island. This encourages the idea that vicinal adatoms are incorporated into the island or alternatively migrate to the subsurface, increasing the oxide thickness. This would also explain the plateau in sticking probability between 2.4 and 3 ML, where chemisorption occurs after the incorporation of adatoms into the oxide layer. The number of free sites for adsorption thus remains constant in this regime and so too does the sticking probability. Subsequently for coverages greater than 3 ML, oxide film growth is the only mechanism, as revealed by the relatively constant heat of adsorption at approximately 260 kJ mol<sup>-1</sup>.

Previous studies of the adsorption of oxygen on different stepped surfaces in the oxidation regime have shown a particular surface reconstruction in which the step height and the terrace width double. This oxygen-driven reconstruction has been observed on Ni{977},<sup>30,31</sup> Cu{211},<sup>9</sup> Ru{0001},<sup>32</sup> Pt{977},<sup>33,34</sup>

(23) Ge, Q.; Hu, P.; King, D. A.; Lee, M.-H.; White, J. A.; Payne, M. C. J. *Chem. Phys.* **1997**, *106*, 1210–1215.

(24) Alavi, A.; Hu, P.; Deutsch, T.; Silvestrelli, P. L.; Hutter, J. *Phys. Rev. Lett.* **1998**, *80*, 3650–3653.

(25) Liu, Z.-P.; Hu, P. *J. Chem. Phys.* **2001**, *115*, 4977–4980.

(26) Yamagishi, S.; Jenkins, S.; King, D. A. *Surf. Sci.* **2003**, *543*, 12–18.

(27) Horgan, A. M.; King, D. A. *Surf. Sci.* **1970**, *23*, 259–282.

(28) Holloway, P. H.; Hudson, J. B. *Surf. Sci.* **1974**, *43*, 123–140.

(29) Bäumer, M.; Cappus, D.; Kühlenbeck, H.; Freund, H.-J.; Wilhelm, G.; Brodde, A.; Neddermeyer, H. *Surf. Sci.* **1991**, *253*, 116–128.

(30) Niu, L.; Koleske, D. D.; Gaspar, D. J.; King, S. F.; Sibener, S. J. *Surf. Sci.* **1996**, *356*, 144–160.

(31) Pearl, T. P.; Sibener, S. J. *J. Chem. Phys.* **2001**, *115*, 1916–1927.

**Table 2.** Comparison of Data Pertaining to the Interaction of Oxygen with Nickel Surfaces in the Oxide Film Growth Regime<sup>a</sup>

|                      | $q_{\text{int}}$ onset/kJ mol <sup>-1</sup> | $\Theta_{\text{ox}}$ onset/O ML | $\Theta_{\text{sat}}$ /O ML |
|----------------------|---|---------------------------------|-----------------------------|
| Ni{211} <sup>b</sup> | 380   | 2.0                             | 9.0                         |
| Ni{100} <sup>c</sup> | 350   | 0.68                            | 3.6                         |
| Ni{110} <sup>c</sup> | 380   | 0.8–1.2                         | 4.1                         |
| Ni{111} <sup>c</sup> | 410   | 0.45                            | 3.0                         |

<sup>a</sup>  $q_{\text{int}}$  onset is the integral heat of adsorption at the oxidation onset,  $\Theta_{\text{ox}}$  onset is the oxygen coverage at the beginning of the oxidation, and  $\Theta_{\text{sat}}$  is saturation coverage at the steady state at 300 K. <sup>b</sup> This work. <sup>c</sup> Data reproduced from ref 21.

and Rh{332},<sup>35</sup> using LEED and scanning tunneling microscopy (STM). However, the common key feature of these studies is the elevated surface temperature at which the reconstruction is observed. On Ni{977}, the double-stepped structure is observed over the temperature range 390–470 K.<sup>30,31</sup> On Cu{211}, the oxygen adlayer is annealed over the temperature range 450–650 K in order to produce double steps, which are stable up to 800 K.<sup>9</sup> On stepped Ru{0001} [ $n\{001\} \times \{010\}$ ] with  $n = 13$  or 39, the same restructuring occurs over the temperature range 500–700 K with stability to 1200 K.<sup>32</sup> Similarly, in the case of Pt{977} the surface was heated in an oxygen environment in the temperature range 600–900 K,<sup>33,34</sup> and in the case of Rh{332}, the doubling of the step height and terrace occurs at surface temperatures between 430 and 510 K.<sup>35</sup> Therefore, in the case of the present study, the drop in the heat of adsorption between 2.4 and 3 ML, which is interpreted as chemisorption on terrace sites in the metastable regime, cannot be ascribed to a similar restructuring, because adsorption is conducted at room temperature.

Table 2 reports the key values for adsorption in the oxide regimes in comparison with those obtained for adsorption on low Miller index Ni surfaces. It is interesting to note that the integral heat at the oxidation onset for Ni{211} at 2 ML is 380 kJ mol<sup>-1</sup>, a value which is very similar to those found for each of the low Miller index nickel surfaces.<sup>21</sup> This would suggest that the transition between chemisorption and oxidation is intrinsically governed by the thermodynamics and the structure of the surface plays no role.

Finally, in the steady state regime, where both the differential heat of adsorption and the sticking probability are relatively independent of coverage,  $q$  is 90 kJ mol<sup>-1</sup> and this is reached

at about 9 ML. This is due to reversible *molecular* adsorption. In this regime, since the amount of molecular oxygen desorbing between molecular beam pulses exactly balances that adsorbing during pulses, the rate of adsorption during the pulse can be equated to the rate of desorption<sup>36</sup> to yield a preexponential factor  $\nu$  for desorption obtained as  $3 \times 10^{12}$  s<sup>-1</sup>. This is in the anticipated range for first-order desorption kinetics.

It is also interesting to note that the steady-state coverage of 9 ML, which corresponds to three O adatoms per exposed Ni atom on the {211} surface, is consistent with the oxygen saturation coverage of 3 ML reported on the {111} surface.<sup>21</sup>

## 5. Conclusions

Using single-crystal adsorption calorimetry we have shown that adsorption of O<sub>2</sub> on stepped Ni{211} is rather complex. Initial dissociative adsorption occurs on the step atoms, revealed by the initial heat of adsorption, which is considerably higher than that of any low Miller index Ni surface. As the coverage increases, one can clearly distinguish the switch from adsorption on steps to adsorption on terraces at 1 ML, the beginning of oxide formation at 2 ML, the metastable regime between 2 and 3 ML, for which oxidation and chemisorption are competitive mechanisms, and a pure oxide film growth regime for coverages greater than 3 ML.

Oxide film formation may be initiated at step sites acting as nucleation points. However, during the first step of oxidation, competition between chemisorption and oxidation can be explained by assuming that oxygen adatoms on the terraces are pulled into the oxide islands, generating free sites on the terraces where further chemisorption may occur. We attribute this to the step atoms where oxygen adatoms are considerably more strongly bound. As the islands get larger, oxidation is the only mechanism, as revealed by the relatively constant heat of adsorption. In the chemisorption regime, models for oxygen dissociative adsorption are proposed for 0.5 and for 1 ML coverage. At this coverage the magnitude of near neighbor lateral pairwise interactions,  $\omega_1$ , and the next nearest neighbor interactions,  $\omega_2$ , are strongly repulsive. These strong interactions in the chemisorbed layer are responsible for the transition to oxide film formation at higher coverages.

**Acknowledgment.** We acknowledge the EPSRC for an equipment grant, postdoctoral support (V.F.) and a research studentship (A.D.K.). Jacques Chevallier of Aarhus University, Denmark, is thanked for providing the thin film single crystal. We also thank Dr. Stephen Jenkins and Dr. Zhi-Pan Liu for fruitful discussions.

JA047165I

- (32) Held, G.; Uremovic, S.; Menzel, D. *Surf. Sci.* **1995**, *333*, 1122–1128.  
 (33) Comsa, G.; Mechttersheimer, G.; Poelsema, B. *Surf. Sci.* **1982**, *119*, 159–171.  
 (34) Comsa, G.; Mechttersheimer, G.; Poelsema, B. *Surf. Sci.* **1982**, *119*, 172–183.  
 (35) Hoogers, G.; King, D. A. *Surf. Sci.* **1993**, *286*, 306–316.  
 (36) Yeo, Y. Y.; Vattuone, L.; King, D. A. *J. Chem. Phys.* **1995**, *104*, 3810–3821.